BIOACTIVE BIOGENOUS MINERAL FOR BONE BONDING APPLICATIONS

Georgiana Dana DUMITRESCU[1], Andrada SERAFIM[*1], Eugeniu VASILE[2], Horia IOVU[1], Izabela Cristina STANCU[1]

In the last years, the interest in using cuttlefish bone in the synthesis of biomaterials with medical applications has increased due to its multifunctional properties, porosity, compressive and flexural strength [1]. This mineral is appealing as bioactive bone substitute due to its composition and micro-structural features and in addition it presents the advantage of high availability and cost efficiency [2]. We investigated the potential of this biogenous mineral to be bioactive with respect to bone integration when used as bone defects filler. To prove this hypothesis, we verify if it is able to induce biomimetic mineralization when incorporated in inert poly(2-hydroxyethyl methacrylate (pHEMA)) hydrogels.

Keywords: cuttlefish bone, mineralization, biodynamic test instrument

1. Introduction

The biomaterials used as fillers in bone regeneration and reconstruction should have a strong binding ability in order to prevent displacement. It has been demonstrated that biomaterials containing hydroxyapatite (either added during synthesis or formed *in vivo*) exhibit an enhanced ability to bind with living bone due to its similarity with host [1].

In the last years, the interest in using cuttlefish bone as filler for scaffolds designed for hard tissue regeneration has increased [2]. As an example, a search using the term "cuttlefish bone" on ScienceDirect database showed that only ten research papers were published in the year 2000 and over sixty in 2018 [3]. This natural material is appealing as bioactive bone substitute due to its composition (a crystallized form of calcium carbonate and chitin [2], [4]) and micro-structural features (porosity, light-weight, compressive and flexural strength [5]) and in addition it presents the advantages of high availability and cost efficiency [6], [7]. The cuttlefish bone has important characteristics: a great biomineralization area and a very large organic matrix [3].

[1] Advanced Polymer Materials Group, Faculty of Applied Chemistry and Materials Science, University POLITEHNICA of Bucharest, Romania
[2] Department of Science and Engineering of Oxide Materials and Nanomaterials, University POLITEHNICA of Bucharest, Bucharest, Romania

The use of cuttlefish bone as a filler in acrylic bone cements was investigated and found enhanced osseointegration and no evidence of secondary infection during *in vivo* testing on rabbits. The mechanical properties of the bone cement with up to 30% cuttlefish bone filler were found to be comparable to those of the commercial bone cement, and well within the accepted standards for bone cements [5],[8].

Another approach for using cuttlefish bone in tissue scaffolding applications revolves around the hydrothermal transformation of aragonite into hydroxyapatite [9]. The studies included tests for biocompatibility with osteoblasts, whose viability was enhanced by the presence of such mineral components. A range of other benefits including good machinability and fluoride substitution for dental applications are also recognized, indicating rather promising results [5],[8].

The ability of a biomaterial to integrate with bone tissue can be evaluated using the simulated body fluid (SBF) test to study *in vitro* formation of Ca/P mineral phase at the surface of a material when immersed in SBF. The SBF solution (originally named simulated physiological solution, SPS [1],[10]) has similar ion concentration to human blood plasma and the test is carried out by maintaining solution pH and temperature to match those of blood plasma, as it has been found that this is required for formation of an apatite mineral [1],[10]. Thus, the ability of a scaffold to replace or repair natural bone tissue may be evaluated based on its ability to form bone-like hydroxyapatite. The test can be performed through immersion in a certain volume of SBF, for a pre-established period of time, as described by Kokubo in [11].

The present study aims the evaluation of the potential of the mineral phase of cuttlefish bone to act as biomimetic mineralization initiator when embedded in an inert polymeric matrix in order to be subsequently used in the field of hard tissue regeneration or repair. In this respect, cuttlefish bone fragments were immobilized into poly(2-hydroxyethyl methacrylate) (samples further referred to as CB-pHEMA) and their mineralization potential was further investigated. Using SBF as incubation media, the study presents two routes of mineralization: the conventional static one and an innovative one in which the incubation is performed under uniaxial compression and continuous flow of SBF. The formation of biomimetic apatite into the pHEMA matrix was explored through Fourier transform infrared (FTIR) spectroscopy. The overall presence of the mineral in the synthesized materials was imagined through micro-computed tomography (micro-CT), while detailed 2D images of thin slices were registered using scanning electron microscopy (SEM).

2. Materials and methods

2.1. Materials

2-hydroxyethyl methacrylate (HEMA) and silver nitrate were purchased from Sigma Aldrich and used as such. Ammonium persulfate (APS) also purchased form Sigma Aldrich was used as initiator in the polymerization reaction. Ethylene glycol dimethacrylate (EGDMA) was purchased from Fluka and used as crosslinker. Cuttlefish bone (CB) was purchased from pet shops in Romania where it is sold as calcium supplement for birds.

For the preparation of SBF, sodium chloride (NaCl), sodium hydrogen carbonate ($NaHCO_3$), potassium chloride (KCl), di-potassium hydrogen phosphate trihydrate ($K_2HPO_4 \cdot 3H_2O$), magnesium chloride hexahydrate ($MgCl_2 \cdot 6H_2O$), calcium chloride ($CaCl_2$), sodium sulfate (Na_2SO_4), Tris-hydroxymethyl aminomethane: ($(HOCH_2)_3CNH_2$) (Tris), 1 M (mol/l) Hydrochloric Acid, 1M-HCl were used according to the protocol described in [11].

2.2. Methods

2.2.1. Synthesis of CB – pHEMA materials

The CB powder was prepared as described in [7]. Briefly, the CB was cut in small fragments and extensively washed with double distilled water for 3 days at room temperature (RT) and subsequently milled to a powder.

CB – pHEMA scaffolds were synthesized through the free radical bulk polymerization of HEMA in the presence of CB powder (composition described in Table 1), using EGDMA as crosslinker (HEMA:EGDMA = 100:1 molar ratio) and APS as radical initiator (HEMA:APS = 100:1 molar ratio), at 60°C. pHEMA was also synthesized and used as a control matrix.

For simplicity, in the denomination of the samples with the highest CB loading incubated in dynamic conditions the letter D will be added at the end, and the letter S will be added to those incubated in static conditions (i.e. pHEMA_S and pHEMA_D, pHEMA-CB10_S and pHEMA-CB10_D, respectively).

Table 1

Compositions of the synthesized materials

Sample	**HEMA:CB (wt%)**
pHEMA	-
pHEMA : CB1	100 : 1
pHEMA : CB2	100 : 2
pHEMA : CB10	100 : 10

2.2.2. Characterization of hybrid materials

Mineralization testing

The potential of the CB to act as promoter of a biomimetic mineralization was evaluated using both static and dynamic conditions.

Static tests were conducted using samples of each composition immersed in simulated body fluid (SBF) following the protocol described in [11].

For dynamic tests, samples were compressed up to two weeks using an ElectroForce 5210 biodynamic test instrument, at a frequency of 1 Hz and a displacement of ± 2 mm in continuous flow of SBF at a flow rate of 0.2 ml/min and a temperature of 37°C (Fig.1, b).

At the end of the incubations, all the samples gently washed with distilled water to remove residual salts and subsequently dried in the oven at 37^0C.

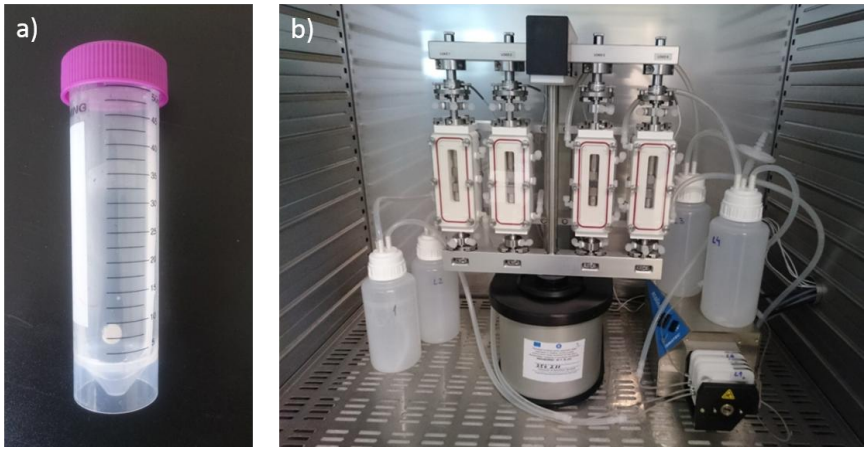

Fig.1. Representative experimental set-up:a) Conventional vial with SBF-incubated sample, b) ElectroForce 5210 biodynamic test instrument

The biodynamic test equipment is appealing for mineralization testing due to the possibility to better simulate natural conditions in the human body: mechanical effort, temperature and dynamic flow of a simulated fluid, such as SBF.

Von Kossa staining

To visually monitor the formation of calcium salts into the CB-containing pHEMA scaffolds after SBF incubation, the samples were immersed into 3 ml silver nitrate solution (1% wt/v), for 60 minutes while being exposed to strong light as described in [12].

Fourier transform infrared (FTIR) analysis

FTIR spectra were recorded using a JASCO 4200 spectrometer equipped with a Specac Golden Gate attenuated total reflectance (ATR) device in the 4000-600 cm^{-1} wavenumber region with a resolution of 4 cm^{-1} and an accumulation of 200 spectra.

Micro-computed tomography (micro-CT)

The micro-CT investigation allowed the comparison of the formation of new mineral phase in dynamic versus static experimental set up. Cylindrical samples dried after the incubation in SBF were scanned. A SkyScan 1272 micro-CT (Bruker) was employed to visualize mineral deposits generated in the polymeric matrix. The equipment uses an X-ray source with peak energies ranging from 20-100 kV. The samples were fixed on the sample holder using modeling clay. All samples were scanned without filter at a voltage of 50 kV and an emission current of 175 µA. The images were registered at a resolution of 2452 x 1640 and a pixel size of 7.0 µm, with a rotation step of 0.4 degrees. All images were processed using CT NRecon software and reconstructed as a 3D object using CTVox.

Morpho-structural characterization

Morphological and microstructural characterization of the hydrogels were performed through scanning electron microscopy (SEM) using QUANTA INSPECT F SEM device equipped with a field emission gun with 1.2 nm resolution and an X-ray energy dispersive spectrometer (EDX). The samples were coated with a thin layer of gold prior to analysis.

3. Results and discussion

The present study aims the evaluation of the potential of the mineral phase of cuttlefish bone to act as biomimetic mineralization initiator when embedded in an inert polymeric matrix (pHEMA) in order to be subsequently used in the field of hard tissue regeneration or repair. In this respect, cuttlefish bone fragments were immobilized into pHEMA and their mineralization was investigated using two experimental conditions: conventional static incubation in SBF and innovative uniaxial compression under continuous flow of SBF.

The scaffolds were obtained as layered structures, containing a pHEMA hydrogel layer (a area in Fig.2) and a composite layer (b area in Fig.2). This design was selected to allow an easy detection of the new mineral formation (if any) in the inert pHEMA layer.

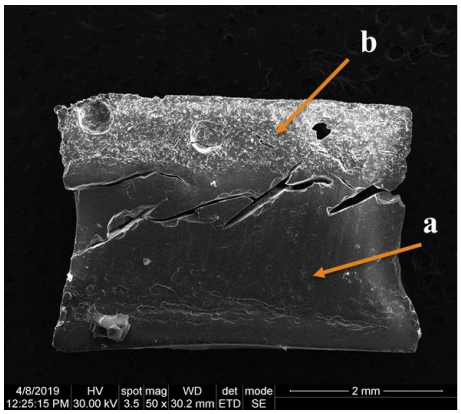

Fig.2. Representative SEM micrograph of a longitudinal section of samplepHEMA-CB10: a – pHEMA matrix, b – composite region containing CB

The scaffolds were subjected to uniaxial compression under continuous flow of SBF and the formation of a new biomimetic mineral phase was investigated through micro-CT, SEM and FTIR spectrometry. The samples did not change their macroscopic appearance during the test. The properties of the synthesized materials were correlated with the biogenous mineral content.

Effect of CB on the mineralization potential

Micro-computed tomography (micro-CT)

Micro-CT images provided microstructural details of the layered samples confirming the precipitation of CB fragments in the pHEMA matrix (Fig.3). The analysis of the samples incubated in SBF revealed different responses in terms of mineralization. When comparing the two types of mineralization tests - static versus dynamic, the micro-CT investigation showed that the mineralization was more efficient in dynamic conditions (Fig.3). The images revealed clusters of newly formed mineral phase in the inert pHEMA hydrogel only in the samples submitted to the biodynamic testing. Such result also confirms our theoretical expectations regarding the relevance of the dynamic evaluation when compared to the static experiments.

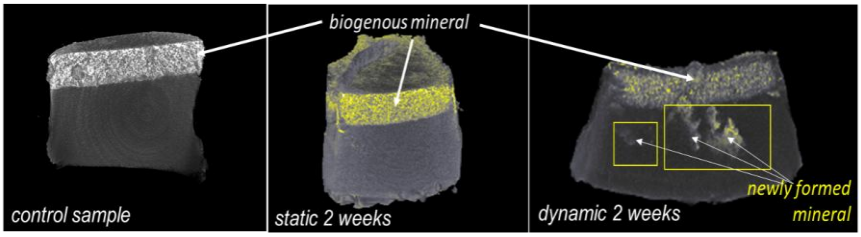

Fig.3. Representative micro-CT images revealing the formation of new mineral phase after 2 weeks incubation in SBF

Staining of the mineral phase

The samples were also subjected to Von Kossa assay before and after incubation in SBF. After two weeks of incubation of the pHEMA-CB10 series, in both static and dynamic set-up, the samples showed a drastic change of color when compared to the non-incubated pHEMA-CB10 sample. The pristine CB-pHEMA sample shows only slight traces of mineral due to the staining of the aragonite from CB fragments (Fig.4, left image - upper row). After incubation in SBF a strong dark brown color can be noticed. Such effect can be assigned to the presence of a denser calcium-containing mineral phase, consisting in CB fragments enriched with newly formed mineral during SBF incubation. It was noticed that the distribution of the new mineral depends on the mineralization test: (i) when static conditions are used, the new mineral phase seems to coexist with the CB fragments (a) and to be localized at the interface (b) with the pHEMA layer while (ii) under dynamic testing, the mineral is formed into the pHEMA layer generating mineralized *walls* with parallel orientation to the longitudinal axis of the applied stress, as visible in Fig.4 (c). Such behavior suggests a stimulation of mineral nucleation and growth in the hydrogel along the stress direction.

The control pHEMA sample doesn't interact with $AgNO_3$ if not immersed in SBF, while after incubation only a low staining is visible due to hydrogel loading with salts form SBF; this effect seems more pronounced when the dynamic incubation was used (the sample is less transparent as visible in Fig.4):

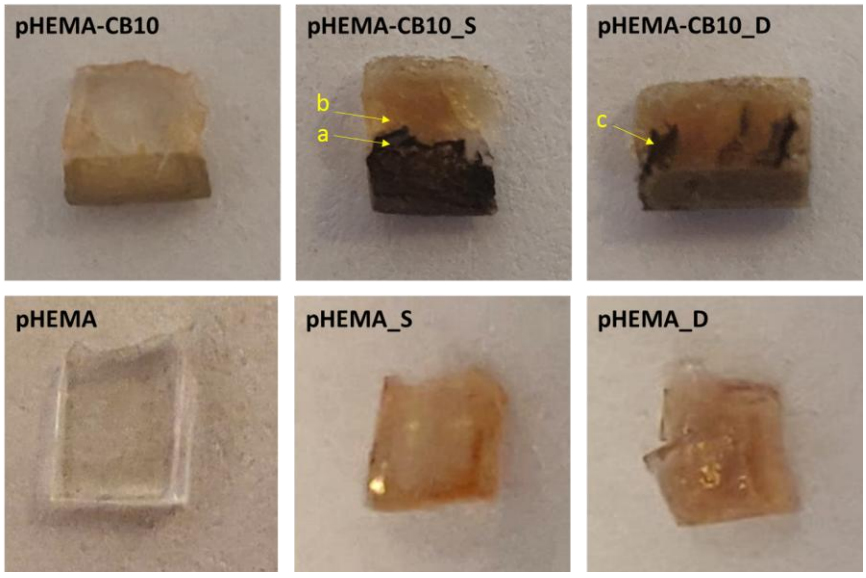

Fig.4. Digital images of the Von Kossa stained samples

These results are in good agreement with the micro-CT images, showing that mineralization testing in dynamic conditions stimulated the formation of mineral.

Fourier transform infrared (FTIR) analysis

The mineralization following incubation in SBF has also been assessed by FTIR analysis. To this end, spectra were registered before and after incubation in SBF. The spectrum of control pHEMA hydrogel displayed typical vibrations at 3490, 2950, 2986, 1713 cm^{-1}, assigned to O-H stretching, C-H symmetric and asymmetric stretching vibrations, as well as to C=O stretching, respectively, of mixed ester and ether origin, while vibrations at 1079cm^{-1} assigned to C-O stretching [13]. The spectra of pHEMA_S and pHEMA_D (Fig.5) are not significantly different when compared to pHEMA:

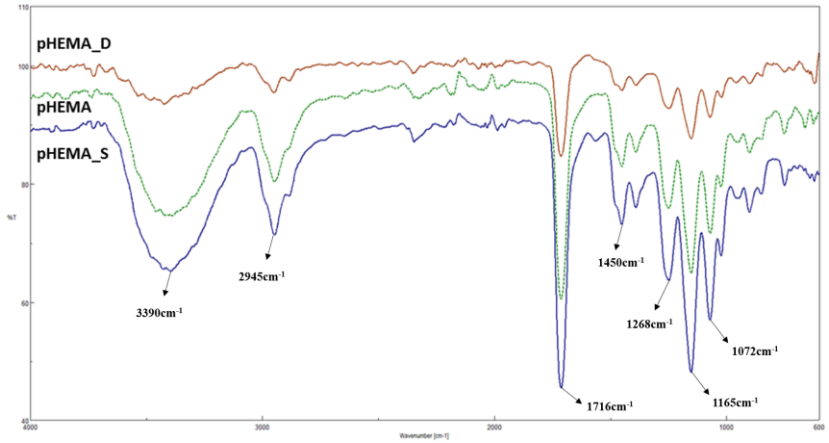

Fig.5. FTIR spectra for pHEMA, pHEMA_S and pHEMA_D

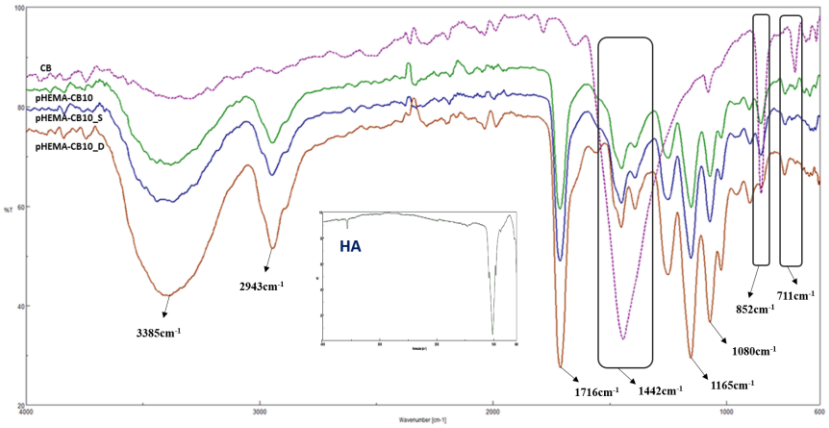

Fig.6. FTIR spectra for pHEMA-CB10, pHEMA-CB10_S, pHEMA-CB10_D and CB. Inset HA-hydroxyapatite spectrum

They do not present signals specific for hydroxyapatite stating for the mineralization inertness of the homopolymer. In the CB-pHEMA samples, aragonite and chitin were detected by FTIR analysis. The spectra were recorded in areas with CB loaded where the mineralization formed. Besides the bands characteristic for aragonite: 1080 cm^{-1}, 711 cm^{-1} and 852 cm^{-1} for C-O in plane band [14], there are bands derived from interval vibrations of CO_3-groups at 1442 cm^{-1} and typical signals from the polymer matrix. A weak contribution to the cuttlefish bone spectrum from chitin is observed in the range 1080 cm^{-1} (C-O stretching). Accordingly, all CB-loaded samples showed typical O-H vibrations at 1716 cm^{-1} (specific for pHEMA spectrum) and the peak characteristic for aragonite at 852 cm^{-1}; the peak specific for chitin, present in the CB at 1080 cm^{-1} is also present in the pHEMA-CB10 samples at 1072 cm^{-1}.

The FTIR spectrum of hydroxyapatite (HA) is shown in the inset in Fig. 6 since it was anticipated that incubation in SBF may lead to generation of newly formed HA. The HA presents O-H-stretching vibration at 3571 cm^{-1} and vibrations of phosphate group at 1020cm^{-1}, 1084cm^{-1}, 961 cm^{-1}, respectively, also bands characteristics for -CO_3 from HA at 899 cm^{-1}, 1450 cm^{-1} and 1623cm^{-1}[15]. All these peaks are visible in the spectral appearance of samples pHEMA-CB10, pHEMA-CB10_S and pHEMA-CB10_D, where CB is incorporated in the polymeric matrix (Fig.6).

Morpho-structural characterization

SEM was used to evaluate the morphology and microstructure of the materials. New mineral was only detected on the samples incubated under dynamic conditions (Fig.7). The microstructure suggests formation of small deposits of nanoapatite during testing.

SEM micrographs indicated that samples incubated under dynamic conditions showed newly formed mineral during the incubation in SBF. Such mineralized phase seems nanostructured (pHEMA-CB10_D panels b,c,e in Fig.7). Samples incubated under static conditions present less evident areas with newly formed mineral, typically developed on the surface of CB fragments, indicating the mineralization occurrence was less intense (pHEMA-CB10_S panels d,e in Fig.7).

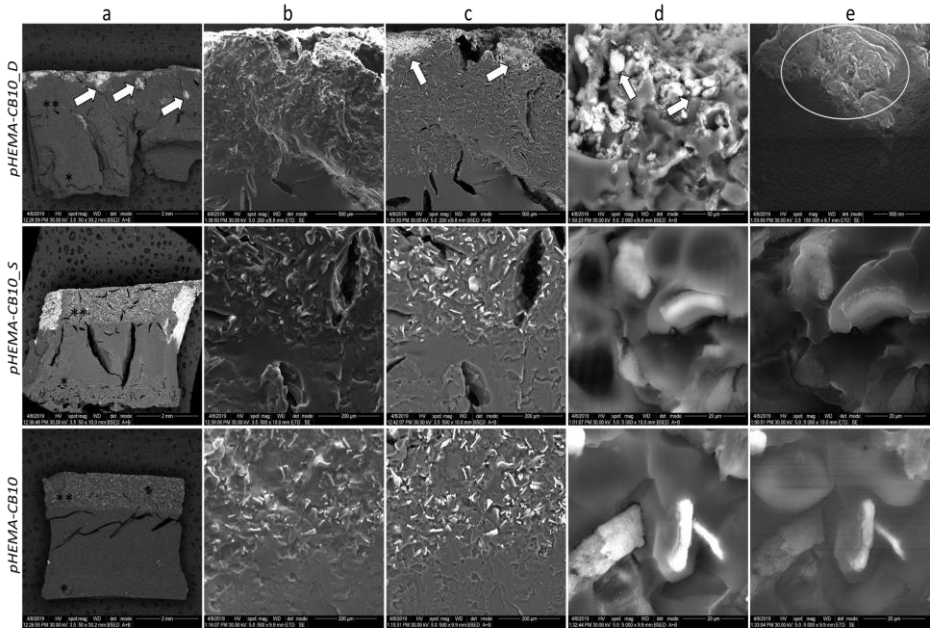

Fig.7. SEM micrographs revealing the influence of the testing conditions (dynamic - D versus static - S) on the mineralization potential of pHEMA-CB10 samples (longitudinal sections); pHEMA-CB10 was used as a control: a – general appearance with two layers (bottom layer (*): pHEMA hydrogel and top layer (**): pHEMA-CB10 composite); b-e – morpho-and microstructural details of the top composite layer in ETD mode – b,e and BSED mode – c,d; white arrow – newly formed mineral during incubation in SBF;
white circle – nanostructured newly formed mineral phase

Fig. 8 provides additional information on the formation and distribution of the newly generated mineral, after incubation, in pHEMA-CB10 samples. The potential of CB to be used as promoter of biomimetic mineralization was confirmed with SEM-EDX mapping. The dynamic testing stimulates more efficient mineralization when compared to static experiments. After dynamic incubation it is observed that a new peak, assigned to phosphate (P) is visible, indicating the formation of a calcium phosphate mineral phase. This is localized as m_2 indicates in Fig.8a. A small peak corresponding for P is also noticed in the EDX spectrum of the static incubated sample (Fig.8b). Elemental SEM-EDX mapping confirms the mineral distribution previously described in the manuscript, namely mineral clusters when dynamic incubation is applied and new formed mineral growing onto CB fragments for the static incubation.

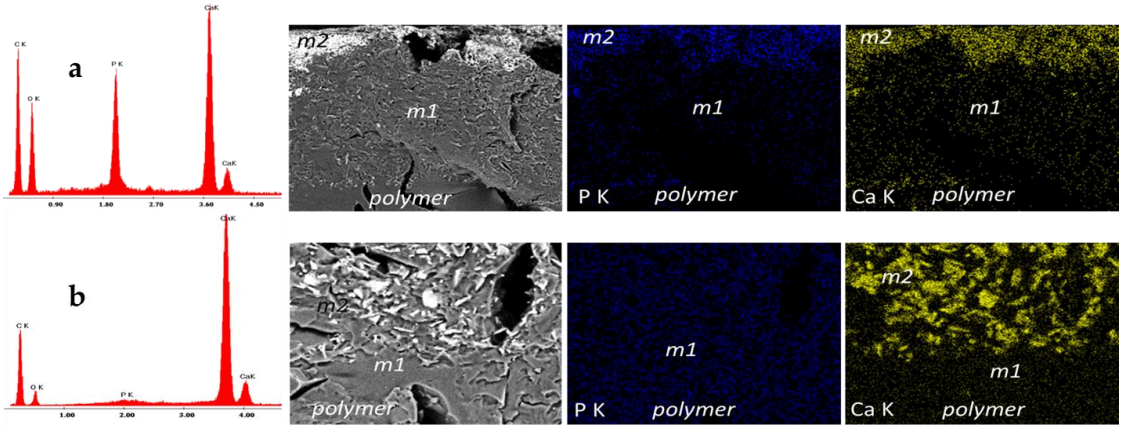

Fig.8. EDX spectra of the testing conditions on the mineralization potential of pHEMA-CB10 samples (longitudinal sections): a) dynamic – D versus b) static – S;
m_1 - pHEMA matrix, m_2 - newly formed mineral

4. Conclusions

The present study aims the evaluation of the potential of the mineral phase of cuttlefish bone to act as biomimetic mineralization initiator when embedded in an inert polymeric matrix in order to be subsequently used in the field of hard tissue regeneration or repair. In this respect, cuttlefish bone fragments were immobilized into pHEMA (samples referred to as CB-pHEMA) and their mineralization was investigated using two experimental conditions: the conventional static incubation in SBF and an innovative uniaxial compression under continuous flow of SBF and.

This study shows the potential of cuttlefish bone to be used as a biogenous mineral. The potential of CB to be used as promoter of biomimetic mineralization was confirmed by FTIR analysis and Von Kossa staining. Also, imaging technologies were employed to visualize the presence of mineral, using both 2D (SEM) and 3D imaging (micro-CT). The dynamic testing stimulates more efficiently the mineralization when compared to static experiments.

Further investigation of the mineralization induced by CB fragments under dynamic conditions will be performed, with mechanical properties monitoring.

Acknowledgement

The utilization of the micro-CT and biodynamic reactor was possible due to European Regional Development Fund through Competitiveness Operational Program 2014-2020, Priority axis 1, ID P_36_611, MySMIS code 107066, INOVABIOMED.

R E F E R E N C E S

[1]. *K. Kepa, R. Coleman, L. Grondahl, In vitro* mineralization of functional polymers, Biosurface and Biotribology, **vol. 1**, 2015, pp. 214-227

[2]. *S. Poompradub, Y. Ikeda, Y. Kokubo, T. Shiono,* Cuttlebone as reinforcing filler for natural rubber, European Polymer Journal, **vol. 44**, 2008, pp. 4157-4164

[3]. *V. Cadez, S.D. Skapin, A. Leonardi, I. Krizaj, S. Kazazic, B. Salopek-Sondi, I. Sondi,* Formation and morphogenesis of a cuttlebone's aragonite biomineral structures for the common cuttlefish (Sepia officinalis) on the nanoscale: Revisited, Journal of Colloid and Interface Science, **vol. 508**, 2017, pp. 95-104

[4]. *L. Vajrabhaya, S. Korsuwannawong, R. Surarit,* Cytotoxic and the proliferative effect of cuttlefish bone on MC3T3-E1 osteoblast cell line, European Journal of Dentistry, **vol. 11**, 2017, pp. 503-507

[5]. *J. Cadman, S. Zhou, Y. Chen, Q. Li,* Cuttlebone: Characterization, Application and Development of Biomimetic Materials, Journal of Bionic Engineering, **vol. 9**, 2012, pp. 367-376

[6]. *J. Cadman, S. Zhou, Y. Chen, W. Li, R. Appleyard, Q. Li,* Characterization of cuttlebone for a biomimetic design of cellular structures, research paper, Acta Mech Sin, **vol. 26**, 2010, pp. 27-35

[7]. *D.M. Dragusin, F. Curti, S. Cecoltan, D. Sarghiuta, L.M. Butac, E. Vasile, R. Marinescu, I.C. Stancu,* Biocomposites based on biogenous mineral for inducing biomimetic mineralization, Materiale Plastice, **vol.54**, no. 2, 2017, pp. 207-213

[8]. *B. Aksakal, M. Demirel,* Synthesis and fabrication of novel cuttlefish (Sepia officinalis) backbone biografts for biomedical applications, Ceramics International, **vol. 41**, 2015, pp. 4531-4537

[9]. *J.H.G. Rocha, A.F. Lemos, S. Kannan, S. Agathopoulos, J.M.F. Ferreira*, Hydroxyapatite scaffols hydrothermally grown from aragonitic cuttlefish bones, Journal of Materials Chemistry, **vol. 15**, 2005, 5007-5011

[10]. *K. Wang, Y. Leng, X. Lu, F. Ren,* Calcium phosphate bioceramics induce mineralization modulated by proteins, Material Science and Engineering, **vol. 33**, 2013, pp. 3245-3255

[11]. *T. Kokubo, H. Takadama,*How useful is SBF in predicting in vivo bone bioactivity? Biomaterials, **vol. 27**, 2006, pp. 2907-2915

[12]. *L.F. Bonewald, S.E. Harris, J. Rosser, M.R. Dallas, S.L. Dallas, N.P. Camacho, B. Boyan, A. Boskey,* Von Kossa Staining Alone is not sufficient to confirm that mineralization *in vitro* represents bone formation, Calcified Tissue International, **vol. 72**, 2003, pp. 537-547

[13]. *E. Vasile, A. Serafim, D.M. Dragusin, C. Petrea, H. Iovu, I.C. Stancu,* Apatite formation on active nanostructured coating based on functionalized gold nanoparticles, Journal of Nanoparticle Research, **vol. 918**, 2012, pp. 1-14

[14]. *D. Chakrabarty, A. Mahapatra,* Aragonite crystals with unconventional morphologies, Journal of Materials Chemistry, vol. 9, 1999, pp. 2953-2957

[15]. *H. Gheisari, E. Karamian, M. Abdellahi,* A novel hydroxyapatite – Hardystonite nanocomposite ceramic, Ceramics International, **vol. 41** (4), 2015, pp. 5967-5975